Acta Crystallographica Section D
Biological Crystallography
ISSN 0907-4449

Nanoflow electrospinning serial femtosecond crystallography

Raymond G. Sierra,[a] Hartawan Laksmono,[a] Jan Kern,[b,c] Rosalie Tran,[b] Johan Hattne,[b] Roberto Alonso-Mori,[c] Benedikt Lassalle-Kaiser,[b] Carina Glöckner,[d] Julia Hellmich,[d] Donald W. Schafer,[c] Nathaniel Echols,[b] Richard J. Gildea,[b] Ralf W. Grosse-Kunstleve,[b] Jonas Sellberg,[e,f] Trevor A. McQueen,[g] Alan R. Fry,[c] Marc M. Messerschmidt,[c] Alan Miahnahri,[c] M. Marvin Seibert,[c] Christina Y. Hampton,[a] Dmitri Starodub,[a] N. Duane Loh,[a] Dimosthenis Sokaras,[e] Tsu-Chien Weng,[e] Petrus H. Zwart,[b] Pieter Glatzel,[h] Despina Milathianaki,[c] William E. White,[c] Paul D. Adams,[b] Garth J. Williams,[c] Sébastien Boutet,[c] Athina Zouni,[d] Johannes Messinger,[i] Nicholas K. Sauter,[b] Uwe Bergmann,[c] Junko Yano,[b] Vittal K. Yachandra[b] and Michael J. Bogan[a,c]*

[a]PULSE Institute, SLAC National Accelerator Laboratory, Menlo Park, CA 94025, USA, [b]Physical Biosciences Division, Lawrence Berkeley National Laboratory, Berkeley, CA 94720, USA, [c]LCLS, SLAC National Accelerator Laboratory, Menlo Park, CA 94025, USA, [d]Max-Volmer-Laboratorium für Biophysikalische Chemie, Technische Universität Berlin, Strasse des 17 Juni 135, 10623 Berlin, Germany, [e]SSRL, SLAC National Accelerator Laboratory, Menlo Park, CA 94025, USA, [f]Department of Physics, AlbaNova, Stockholm University, S-106 91 Stockholm, Sweden, [g]Department of Chemistry, Stanford University, Stanford, CA 94025, USA, [h]European Synchrotron Radiation Facility, Grenoble, France, and [i]Institutionen för Kemi, Kemiskt Biologiskt Centrum, Umeå Universitet, Umeå, Sweden

Correspondence e-mail: mbogan@slac.stanford.edu

Received 24 July 2012
Accepted 5 September 2012

An electrospun liquid microjet has been developed that delivers protein microcrystal suspensions at flow rates of 0.14–3.1 µl min^{-1} to perform serial femtosecond crystallography (SFX) studies with X-ray lasers. Thermolysin microcrystals flowed at 0.17 µl min^{-1} and diffracted to beyond 4 Å resolution, producing 14 000 indexable diffraction patterns, or four per second, from 140 µg of protein. Nanoflow electrospinning extends SFX to biological samples that necessitate minimal sample consumption.

1. Introduction

Since the first investigation of protein crystals using synchrotron radiation, intense X-ray sources have been powerful tools for structural biology. However, damage owing to X-ray radiation limits the achievable resolution, especially for proteins containing redox-active (metal) cofactors (Henderson, 1995; Yano *et al.*, 2005). While specialized cryogenic cooling methods have helped to maximize data collection before the onset of damage, the advent of short-pulse X-ray free-electron lasers (XFELs) offers a completely new crystallographic paradigm by enabling serial femtosecond crystallography (SFX). Diffraction patterns from millions of individual protein microcrystals can be captured one at a time before X-ray damage manifests itself (Chapman *et al.*, 2011). SFX using the Coherent X-ray Imaging (CXI) endstation (Boutet & Williams, 2010) at the Linac Coherent Light Source (LCLS) has already produced high-resolution (<2 Å) protein structures (Boutet *et al.*, 2012). In this brief communication, we report a sample-delivery method that reduces sample consumption by 60–100 times compared with the current method (DePonte *et al.*, 2008) while meeting the unique needs of SFX for structural biology.

In SFX, the intense LCLS pulses destroy the sample with every shot; therefore, crystals must be replenished at 120 Hz, the laser repetition rate. Crystals sized 0.2–20 µm are dispersed in aqueous solutions at concentrations of about 10^9 crystals ml^{-1} and are delivered from a reservoir to the X-ray-interaction region through 40–100 µm internal diameter (ID) silica capillaries. Once the suspension arrives at the X-ray-interaction region, a thin liquid jet (microjet) created at the capillary exit minimizes the thickness of carrier solvent surrounding the microcrystals to reduce background scattering and to improve Bragg peak detection.

The first SFX experiments utilized a gas dynamic virtual nozzle (GDVN; DePonte *et al.*, 2008) to generate the microjet. The GDVN injects a microjet into vacuum using a gas sheath for flow focusing. X-rays probe the jet either within the continuous jet at the capillary exit or further downstream where the jet breaks up into monodisperse droplets because of Rayleigh instability (DePonte *et al.*, 2008). The GDVN is a highly successful tool for SFX experiments (Koopmann *et al.*, 2012; Johansson *et al.*, 2012; Boutet *et al.*, 2012; Aquila *et al.*, 2012; Lomb *et al.*, 2011; Chapman *et al.*, 2011; Barty *et al.*, 2011; Weierstall *et al.*, 2012). Reduction of the 10–16 µl min^{-1} sample-consumption rate, which makes data collection for many precious

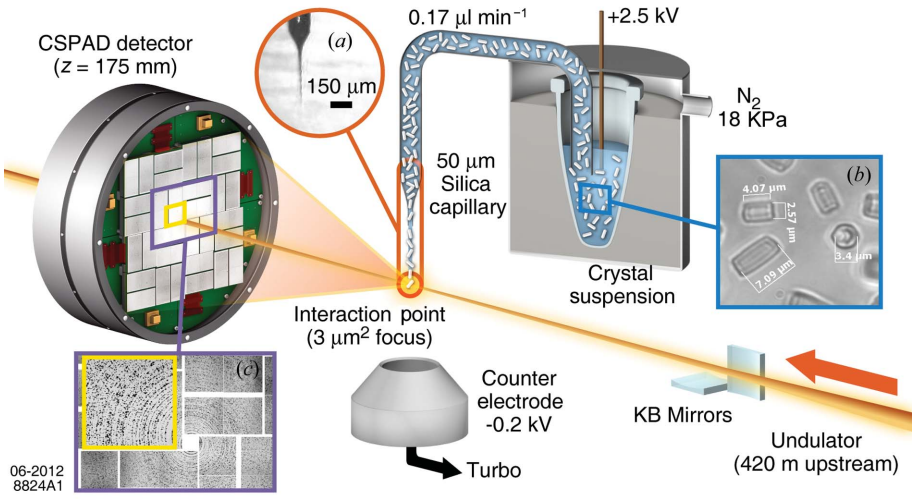

Figure 1
Nanoflow electrospinning protein microcrystal suspensions *in vacuo* for serial femtosecond crystallography at the LCLS Coherent X-ray Imaging endstation. An electrospun microjet (*a*) (scale bar 150 µm) of a thermolysin crystal suspension (*b*) (microscope image) flowing at 0.17 µl min^{-1} is emitted in an electrospun microjet from a 50 µm internal diameter silica capillary positioned <1 mm from the X-ray-interaction point. An average of 2 mJ is delivered in each 40 fs pulse of 9.7 keV X-rays. Single-pulse diffraction patterns from single crystals were recorded on a Cornell-SLAC Pixel Array Detector (CSPAD). A virtual powder pattern from 1024 LCLS shots that produced ≥16 Bragg peaks each (*c*) showed diffraction beyond 4 Å resolution. Purple and yellow squares denote the portions of the CSPAD shown in the virtual powder pattern.

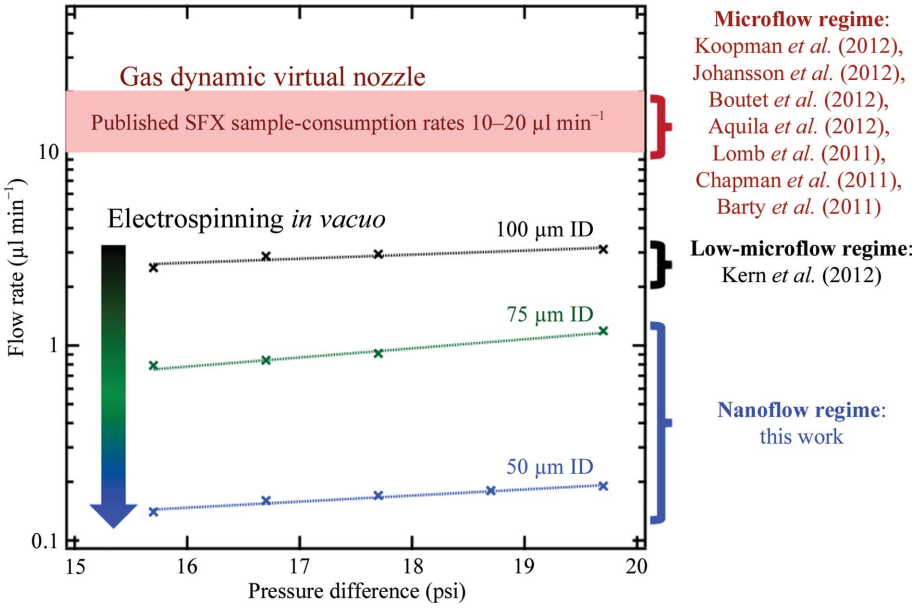

Figure 2
Tuning the sample flow rate of electrospun microjets into the nanoflow regime using capillary internal diameter (ID) and the pressure difference between the liquid reservoir and the vacuum chamber. The sample flow rate was measured for 30%(*w*/*v*) glycerol, 10%(*w*/*v*) PEG 2000, pH 6.5, 5 m*M* $CaCl_2$, 100 m*M* MES buffer solution emitted into vacuum from 50, 75 and 100 µm ID silica capillaries that were 114, 110 and 120 cm long, respectively. Linear fits are added to aid the eye. The range of flow rates for published SFX experiments is highlighted for comparison but note that the GDVN operates with higher backing pressure on the liquid than the values on the abscissa.

biological samples costly and demanding, is paramount to broadening the applicability of SFX.

2. Results and discussion

LCLS fires at 120 Hz and therefore protein passing through the microjet is wasted during the 8.3 ms delay between shots. Sample consumption could be reduced during SFX if a microjet could be formed with the same diameter but using a lower flow rate, since less unused sample is passed through the interaction region between two X-ray pulses: 1.4 nl of sample passes between each pulse at 10 µl min^{-1}, whereas only about 0.028 nl is wasted at 0.2 µl min^{-1}. In our recent SFX study of photosystem II (Kern *et al.*, 2012), we utilized an electric field-focused microjet operated at 2.5–3.1 µl min^{-1} that is described below.

The physics of gas and electric field flow focusing lead to comparable microjet formation (Ganan-Calvo & Montanero, 2009), suggesting that electrospray methodology may be an alternative approach for crystal suspension delivery for SFX. Electrosprays are formed when a sufficiently high electric field overcomes the surface tension and focuses the free surface of a liquid into a microjet, which breaks apart into highly charged droplets shortly after (Ganan-Calvo & Montanero, 2009). The potential use of droplet beams produced from electrospray voltage-assisted Rayleigh microjets in SFX has been studied (Weierstall *et al.*, 2007). However, concerns exist regarding the high divergence of the droplet stream and the potential impact of the electric field on the biomolecular structure in the small charged droplets emitted (DePonte *et al.*, 2008; Fromme & Spence, 2011; Shapiro *et al.*, 2008).

In our nanoflow SFX sample-delivery system, instead of creating diverging droplet streams of protein crystals using an electrospray we apply a principle utilized in electrospinning (Fridrikh *et al.*, 2003), in which the length of the microjet is extended and droplet formation is delayed by adding glycerol and/or polyethylene glycol (PEG). The aim is to keep the crystals inside a focused liquid stream for as long as possible to ensure X-ray probing before potentially spurious effects owing to droplet formation can occur. Varying the onset and geometry of the electrospun microjet formed downstream of a fixed capillary ID is achieved by varying the flow rate and the applied electric field (Fridrikh *et al.*, 2003).

For the operation of our electrospun microjet at CXI, where SFX is performed at <0.01 Pa in order to minimize background scattering, stable operating parameters outside the typical atmospheric pressure conditions were developed. Pure glycerol, which is commonly used in crystal screens and as a cryoprotectant in synchrotron protein crystallography, electrosprays stably below 0.01 Pa (Ku & Kim, 2003). We observed that aqueous glycerol solutions at 25–40%(*w*/*v*) produced stable electrospun microjets at <1 Pa. Similarly, electrospun microjets of crystal suspensions in glycerol–water mixtures showed excellent stability at

pressures below 0.01 Pa, operating well outside the corona discharge regime (Ku & Kim, 2003).

The compatibility of electrospinning with crystal suspensions that contain dense additives such as glycerol adds the advantage that the crystals settle at a slower rate. Protein-crystal settling during sample-line transit or during storage in a reservoir reduces the acquisition rate of useful data in SFX by decreasing the crystal concentration in the X-ray-interaction region (Weierstall *et al.*, 2012; Lomb *et al.*, 2012). It also increases the likelihood of aggregate formation, which can clog the sample-transfer line. The crystal suspensions used in our experiment did not visibly settle for over 12 h, which is longer than the length of a typical beamtime shift at LCLS. One caveat to this approach is that the crystals must be stable in the presence of the glycerol, or other additive, used to mitigate settling.

Nanoflow electrospinning SFX was tested at the LCLS CXI endstation (Fig. 1 and Supplementary Figs. 1–3[1]). An aqueous suspension of thermolysin crystals (Fig. 1*a* and Supplementary Fig. 4[1]) was prepared in a crystallization buffer consisting of 40%(*w*/*v*) PEG 2000, 100 m*M* MES pH 6.5. The microcrystals were then exchanged stepwise into buffer consisting of 30%(*w*/*v*) glycerol with 10%(*w*/*v*) PEG 2000, 100 m*M* MES pH 6.5, 5 m*M* $CaCl_2$. A 100 µl aliquot was filtered through an 8 µm Nucleopore membrane into a micro-centrifuge tube. The tube was loaded into a pressurized cell which established fluid transfer into the SFX vacuum chamber *via* a 114 cm long 50 µm internal diameter × 150 µm outer diameter silica capillary and also established electrical contact between the sample suspension and a platinum electrode. A +2.5 kV potential was applied to the platinum electrode and −0.2 kV was applied to a counter electrode positioned 5–8 mm from the capillary exit, resulting in electric fields between 3400 and 5400 V cm^{-1}. The sample-delivery rate was tuned to 0.17 µl min^{-1} by varying the N_2 backing pressure applied to the solution and the capillary internal diameter (Fig. 2 and Supplementary Table 1[1]).

The microcrystal diffraction data in Fig. 1 indicate that nanoflow electrospinning is suitable for SFX and the presence of the electric field has no discernible impact on the crystal integrity as diffraction beyond 4 Å resolution was observed. In 1 h, about 14 000 single-shot diffraction patterns with ≥16 Bragg peaks were recorded from individual thermolysin microcrystals. A portion of the data (1024 shots) is shown in Fig. 1(*c*) as a virtual powder pattern (the full pattern is shown in Supplementary Fig. 5[1]).

A total of 10 µl of 14 mg ml^{-1} thermolysin sample, or 140 µg protein at about 2×10^{10} crystals ml^{-1}, was consumed to collect these data. It is difficult to make a direct comparison with previous SFX experiments owing to the use of different protein crystals, microjets and beamline parameters. SFX of photosystem I (PSI) using a GDVN consumed 5.1 ml of 1 mg ml^{-1} solution at 1×10^9 crystals ml^{-1} to produce 112 725 crystal diffraction patterns with ≥10 Bragg peaks (Chapman *et al.*, 2011). Thus, at 1.1×10^5 patterns mg^{-1}, or one diffraction pattern per 1.4×10^4 crystals, our nanoflow electrospinning SFX experiment is comparable to the 2.2×10^4 patterns mg^{-1}, or one pattern per 4.6×10^4 crystals, collected on PSI at a higher flow rate, even while applying a more stringent selection criterion for Bragg peak detection.

Electrospinning protein-microcrystal suspensions can produce *in vacuo* liquid jets that consume sample at nanolitres per minute and have microscale dimensions. This method thereby provides a complementary sample-delivery mechanism for SFX using X-ray lasers (Supplementary Table 2[1]). Currently, a disadvantage of the electrospun microjet is its sensitivity to freezing with high-water-content solutions. Capillary heating and/or the use of cryoprotectants overcome this issue. Electrospun microjets have several features that are valuable for SFX experiments: simple design, a low flow rate (0.14–3.1 µl min^{-1}), a small sample volume (≥25 µl) delivered from a microcentrifuge tube, low backing pressure applied to the protein crystal sample, the lack of sheath gas, less sample settling owing to compatibility with highly viscous solutions (3–5 cP) and compatibility with the experimental geometries required for pump-probe (Aquila *et al.*, 2012) or X-ray emission spectroscopy experiments (Alonso-Mori *et al.*, 2012). Nanoflow microjets will help to open SFX to a wider array of structural biology problems, including large membrane-protein complexes such as photosystem II (Kern *et al.*, 2012), and provide a means for low-flow sample delivery to a variety of X-ray laser experiments on precious samples.

The nanoflow liquid microjet work was supported by the AMOS program, Office of Science, Office of Basic Energy Sciences (OBES), Division of Chemical Sciences, Geosciences and Biosciences (CSGB) of the Department of Energy (DOE) (MJB), LCLS (MJB and DWS) and through the SLAC Laboratory Directed Research and Development Program (MJB and HL). This work was also supported by OBES, CSGB of the DOE under Contract DE-AC02-05CH11231 (JY and VKY) for structural studies and instrumentation, Director, Office of Science, DOE under Contract DE-AC02-05CH11231 (NKS) for data-processing methods and NIH Grant GM 55302 (VKY) for PS II biochemistry. In addition, the DFG-Cluster of Excellence 'UniCat' coordinated by the Technische Universität Berlin (AZ), the Solar Fuels Strong Research Environment (Umeå University; JM), the Artificial Leaf Project (K&A Wallenberg Foundation; JM) and VR (JM) are acknowledged for supporting this project. Experiments were carried out at the LCLS at SLAC National Accelerator Laboratory operated by Stanford University on behalf of DOE, OBES. We thank the staff at LCLS/SLAC for their support.

References

Alonso-Mori, R. *et al.* (2012). Submitted.
Aquila, A. *et al.* (2012). *Opt. Express*, **20**, 2706–2716.
Barty, A. *et al.* (2011). *Nature Photonics*, **6**, 35–40.
Boutet, S. *et al.* (2012). *Science*, **337**, 362–364.
Boutet, S. & Williams, G. (2010). *New J. Phys.* **12**, 035024.
Chapman, H. N. *et al.* (2011). *Nature (London)*, **470**, 73–77.
DePonte, D. P., Weierstall, U., Schmidt, K., Warner, J., Starodub, D., Spence, J. C. H. & Doak, R. B. (2008). *J. Phys. D Appl. Phys.* **41**, 195505.
Fridrikh, S. V., Yu, J. H., Brenner, M. P. & Rutledge, G. C. (2003). *Phys. Rev. Lett.* **90**, 144502.
Fromme, P. & Spence, J. C. H. (2011). *Curr. Opin. Struct. Biol.* **21**, 509–516.
Ganan-Calvo, A. M. & Montanero, J. M. (2009). *Phys. Rev. E*, **79**, 066305.
Henderson, R. (1995). *Q. Rev. Biophys.* **144**, 171–193.
Johansson, L. C. *et al.* (2012). *Nature Methods*, **9**, 263–265.
Kern, J. *et al.* (2012). *Proc. Natl Acad. Sci. USA*, **109**, 9721–9726.
Koopmann, R. *et al.* (2012). *Nature Methods*, **9**, 259–262.
Ku, B. K. & Kim, S. S. (2003). *J. Electrostat.* **57**, 109–128.
Lomb, L. *et al.* (2011). *Phys. Rev. B*, **84**, 214111.
Lomb, L., Steinbrener, J., Bari, S., Beisel, D., Berndt, D., Kieser, C., Lukat, M., Neef, N. & Shoeman, R. L. (2012). *J. Appl. Cryst.* **45**, 674–678.
Philipp, H. T., Hromalik, M., Tate, M., Koerner, L. & Gruner, S. M. (2011). *Nucl. Instrum. Methods Phys. Res. A*, **649**, 67.
Shapiro, D. A., Chapman, H. N., DePonte, D., Doak, R. B., Fromme, P., Hembree, G., Hunter, M., Marchesini, S., Schmidt, K., Spence, J., Starodub, D. & Weierstall, U. (2008). *J. Synchrotron Rad.* **15**, 593–599.
Weierstall, U., Doak, R. B., Spence, J. C. H., Starodub, D., Shapiro, D., Kennedy, P., Warner, J., Hembree, G. G., Fromme, P. and Chapman, H. N. (2007). *Exp. Fluids*, **44**, 675–689.

[1] Supplementary material has been deposited in the IUCr electronic archive (Reference: LV5021). Services for accessing this material are described at the back of the journal.

Weierstall, U., Spence, J. C. H. & Doak, R. B. (2012). *Rev. Sci. Instrum.* **83**, 035108–035112.
Yano, J., Kern, J., Irrgang, K. D., Latimer, M. J., Bergmann, U., Glatzel, P., Pushkar, Y., Biesiadka, J., Loll, B., Sauer, K., Messinger, J., Zouni, A. & Yachandra, V. K. (2005). *Proc. Natl Acad. Sci. USA*, **102**, 12047–12052.